Pis'ma v ZhETF, vol. 102, iss. 8, pp. 596 – 601

Anomalous behavior of dielectric response of quantum paraelectric $CaTiO_3$ with iron impurities

E. A. Popova[+*1)], *E. A. Rumyantseva*[+], *B. Kh. Khananov*[+], *V. G. Zalessky*[+], *S. V. Krivovichev*[*], *S. G. Lushnikov*[+*]

[+]*Ioffe Institute, 194021 St. Petersburg, Russia*

[*]*Department of Crystallography, St. Petersburg State University, 199034 St. Petersburg, Russia*

Submitted 30 July 2015

Resubmitted 24 August 2015

Herein we report on the studies of lattice dynamics and crystal structure of natural perovskite with the general formula $CaTiO_3$:0.01Fe by dielectric spectroscopy and X-ray diffraction in a wide temperature range. In contrast to the "chemically pure" synthetic perovskite, the lattice dynamics of the Fe-containing natural sample exhibits a structural instability in the vicinity of 240 K. Our studies of the behavior of magnetic moment of $CaTiO_3$:0.01Fe demonstrate that in the temperature region from 4.3 to 300 K this material is paramagnetic. No changes in the crystal symmetry have been observed in the structural studies, which can be explained by the small degree of lattice distortions, as has been observed previously for isotopically substituted $SrTiO_3^{18}$. Conductivity measurements and analysis of the dielectric response dispersion of $CaTiO_3$:0.01Fe have shown that the dispersion is due to the Maxwell–Wagner mechanism and can be attributed to oxygen vacancies present in the mineral.

DOI: 10.7868/S0370274X15200102

Investigations of the dynamics of phase transitions in the crystals of the perovskite family with the common formula ABO_3 and the effects of disorders of various kinds (introduction of ions with different valences into the A or B sublattice, impurities, defects, etc.) are a "hot spot" in the physics of condensed matter. Structural changes associated with ferroelectric phase transitions in perovskites are typically caused by the condensation of one or more modes. As experimental and theoretical studies have shown [1–6], the competition between rotational soft modes corresponding to the rotation of rigid BO_6 octahedra around different crystallographic axes and polar soft modes associated with the displacements of the A and B cations often results in complex sequences of structural transitions. An example of a nontrivial lattice dynamics of perovskites was reported for the group of so-called incipient or quantum paraelectrics such as $SrTiO_3$, $KTaO_3$, $CaTiO_3$, etc. [7–11]. A characteristic feature of the crystal lattice dynamics, owing to which these compounds are regarded as a separate group, is a negative Curie–Weiss temperature. The inverse permittivity in the low-temperature phase obeys the Curie–Weiss law, but does not reach the minimum at the absolute temperature scale. The main reason for this is the competition between order parameters from the R and M points of the Brillouin zone corresponding to the competition between rotational and polar soft modes and an additional contribution of quantum fluctuations. One of the least studied representatives of quantum paraelectrics is natural perovskite, $CaTiO_3$, which gave name to the whole family of crystals with the common formula ABO_3. Whereas synthetic perovskites are studied fairly well, dielectrical properties of natural samples received relatively less attention. It is known that at high temperatures ($T > 1580$ K) perovskite is cubic, space group $Pm\bar{3}m$. Under decreasing temperature, $CaTiO_3$ undergoes a sequence of antiferrodistortive phase transitions (the most probable sequence is $Pm\bar{3}m \to I4/mcm \to Cmcm(\text{or } Imma) \to Pnma)$), the temperatures of which and symmetries of some intermediate phases have not yet been unambiguously established [12–15]. At $T < 1380$ K structural distortions stabilize in the orthorhombic symmetry, space group $Pnma$, $a = 5.444$, $b = 7.644$, $c = 5.367$ Å, $Z = 4$ [12, 15]. All the low-symmetry distortions are caused by the condensation of soft modes from the R and M points of the cubic Brillouin zone and the secondary order parameters [16]. Permittivity in $CaTiO_3$ grows nonlinearly as temperature decreases from room to liquid helium temperature [7]. In the vicinity of 40 K it is saturated, but the crystal nevertheless does not transform into a polar phase state. There is no dispersion of the dielectric response. From the point of view of the crystal lattice dynamics, such a behavior of a static dielectric permit-

[1)]e-mail: elena.popova566@gmail.com

tivity implies that the lattice instability in the form of a polar soft mode is present in $CaTiO_3$ and that it has a tendency to undergo a ferroelectric phase transition. This was confirmed by the temperature behavior of phonon modes in the infrared reflection spectra [17]. In general, perovskites that exhibit the lattice dynamics of this type in the low-temperature region are classified as incipient ferroelectrics. In many cases the introduction of impurity or an isotopic substitution leads to the change in the low-temperature lattice dynamics of virtual ferroelectrics, i.e., the emergence of a ferroelectric phase, antiferroelectric state, etc. [11, 18, 19]. Of particular interest is the lattice dynamics of natural perovskites, which are known to contain impurities, and thus additional phases and modifications of the lattice dynamics can be expected.

The objects of our studies were single crystals of perovskite ($CaTiO_3$:0.01Fe) from the chloritic rock veins of the Perovskitovaya Mine (Kusinsky district, Chelyabinsk region, the Southern Urals, Russia). The samples were found in the form of separate cubic crystals from 0.1 to 2 cm in size and their intergrowths. The crystals were non-transparent and had a grayish-black color. Chemical analysis of the samples demonstrated that the mineral had an iron impurity, the general formula being $CaTiO_3$:0.01Fe. The high-quality crystals were cut along the pseudocubic (001) plane and polished. The samples used for the experiments were platelets $\sim 9 \times 7 \times 1.5\,\text{mm}^3$ in size. The polished crystal faces were coated with gold electrodes by thermal sputtering. The real and imaginary parts of dielectric response were measured by a Good Will LCR-819 impedance meter in the frequency range from 12 Hz to 100 kHz, the amplitude was set to 1.5 V. The temperature dependences were measured in the regime of heating in a dry nitrogen atmosphere in the temperature interval 78–450 K with a constant speed of 1 K/min. To study dielectric hysteresis loops, the Sawyer–Tower scheme was used, the temperature interval was 115–330 K, the field was varied from 0 to 15 kV/cm and the frequency was 50 Hz. The process could be stopped to stabilize temperature with an accuracy of ± 0.2 K. The dc conductivity (the leakage current at zero frequency) was measured by a E6-13A teraohmmeter under voltages of up to 100 V.

Results of measurements of dielectric response and conductivity in $CaTiO_3$:0.01Fe are presented in Figs. 1–3. The temperature range of interest can be conditionally divided into two parts. In the first region, $78\,\text{K} < T < 200\,\text{K}$, the temperature dependence of the real part of the dielectric response is frequency-independent and coincides with that of the synthetic chemically pure

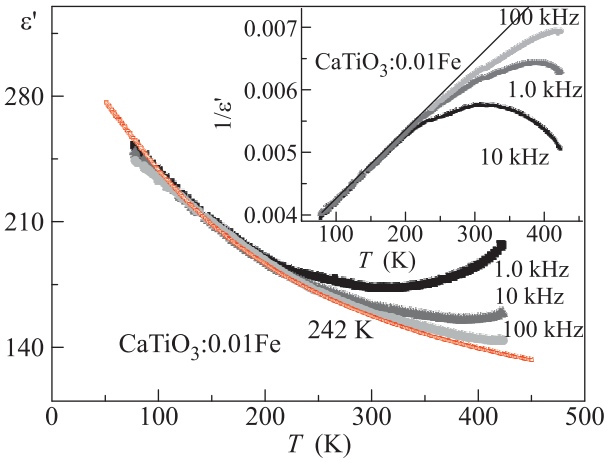

Fig. 1. Temperature dependence of the real part of dielectric response in $CaTiO_3$:0.01Fe at different frequencies. The inset shows temperature dependences of the inverse value of dielectric response at different frequencies (the thin solid line shows the approximation using the Curie–Weiss law)

perovskite (see Fig. 1). It can be seen from Fig. 1 that the decrease in temperature results in a nonlinear increase in $\varepsilon'(T)$, which is more pronounced for the synthetic pure perovskite. The temperature dependence of the imaginary part of the dielectric response exhibits a weak frequency dispersion in the temperature region being analyzed.

As temperature grows, the $\varepsilon'(T)$ dependence exhibits an anomaly in the vicinity of 240 K (see the inset to Fig. 1). Changes in $\varepsilon'(T)$ are small ($\Delta\varepsilon' \sim 1$), but the anomaly is observed at all frequencies. The anomalous behavior of the imaginary part of the dielectric response (Fig. 2) that vanishes at low frequencies is also observed at this temperature.

This anomaly in the dielectric response is masked by dispersion which increases with the increasing frequency and temperature (Figs. 1 and 2).

The growth in $\varepsilon''(T)$ at high frequencies and temperatures is apparently due to the increase in the dc conductivity σ_{dc}. The measured conductivity is shown in Fig. 3. It can be seen from the graph plotted in the $ln\sigma$ vs $1/T$ scale that the conductivity at temperatures above 242 K obeys the Arrhenius law with the activation energy of 0.26 eV. Below this temperature a deviation from this law is observed. The magnitude of the imaginary part of the dielectric response is determined by the sum of dc and ac conductivities $\varepsilon''(T) \sim \sigma_{\text{dc}}/\omega + \omega_{\text{ac}}(\omega)/\omega$. At high temperatures the contribution of σ_{dc} dominates, which results in the significant increase in $\varepsilon''(T)$ [20]. Indeed, the calculations show that above 350 K the behavior of the imaginary

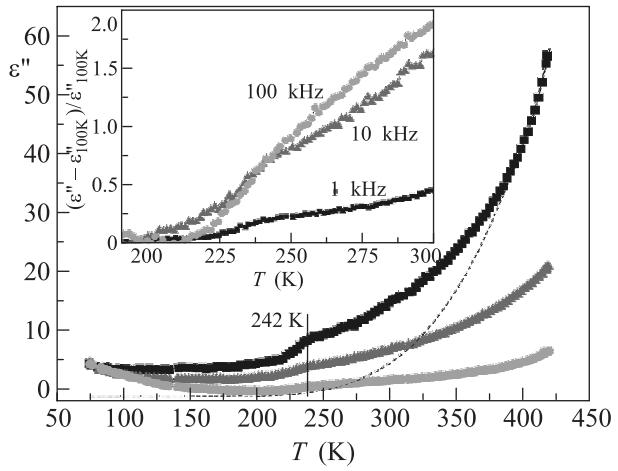

Fig. 2. Temperature dependence of the imaginary part of dielectric response in $CaTiO_3$:0.01Fe. The dotted line shows the temperature behavior of $\varepsilon''(T)$ calculated for the activation energy of 0.22 eV close enough to the activation energy for dc-conductivity. The inset shows temperature dependences in the vicinity of 240 K on an enlarged scale

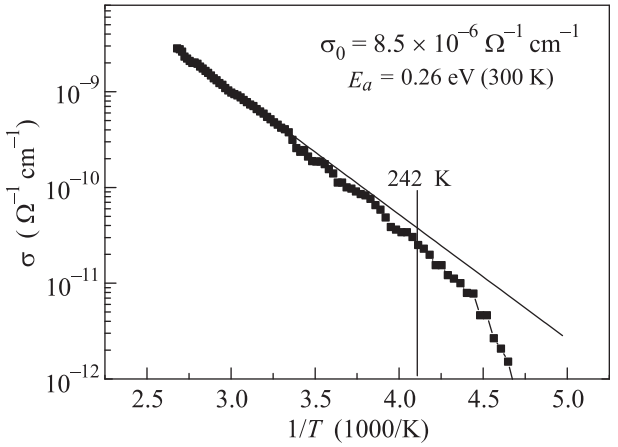

Fig. 3. Temperature dependence of dc conductivity in $CaTiO_3$:0.01Fe

part of the dielectric response at a frequency of 100 kHz is governed by the behavior of conductivity (marked by a dotted line in Fig. 2). This indicates that the high-temperature growth of the real part of the dielectric response simultaneous with the growth in its dispersion is attributable to the Maxwell–Wagner relaxation mechanism. Apparently, one of basic sources of relaxation are oxygen vacancies, the existence of which in perovskite minerals is due to the specific features of its crystallization under natural conditions [15, 21].

Let us return to the dielectric response anomaly in the vicinity of 240 K. Analysis of dielectric hysteresis loops does not reveal a behavior typical for the existence of spontaneous polarization below 240 K. Fig. 1 shows temperature dependences of the inverse value of the real part of the dielectric response in natural perovskite mineral. It is evident that it obeys the Curie–Weiss law below 200 K. The Curie temperature obtained for the inverse value of the real part of the dielectric response in $CaTiO_3$:0.01Fe from the Curie–Weiss law is $T_c = -111$ K, which agrees with the value reported for the chemically pure (synthetic) perovskite.

It is known that in some cases iron impurities in dielectrics can induce unusual magnetic properties. For this reason we measured magnetic properties of $CaTiO_3$:0.01Fe by a Physical Property Measurement System (PPMS). The behavior of the magnetic moment in the temperature range from 4.3 to 300 K under applied magnetic field taken in the field-cooled (FC) and zero field-cooled (ZFC) protocols is presented in Fig. 4. Analysis of the field and temperature measurements

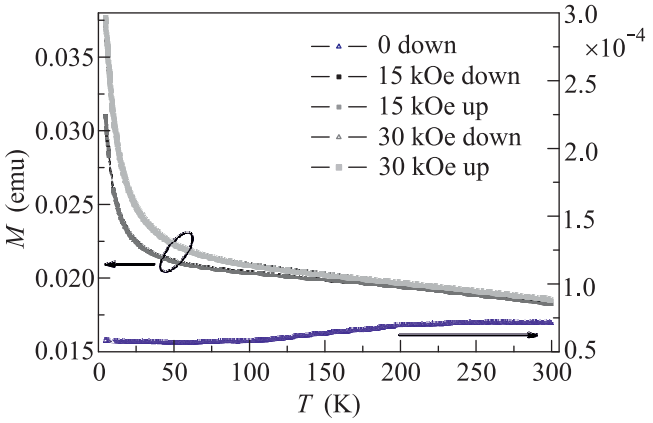

Fig. 4. Temperature dependence of magnetic moment at different applied magnetic filed in $CaTiO_3$:0.01Fe in standard ZFC and FC protocols

showed that $CaTiO_3$: 0.01Fe is a paramagnetic with no anomalies in the behavior of the magnetic moment in various cooling and heating (in the field, without the field) regimes.

Thus, the anomaly in the behavior of the dielectric response of $CaTiO_3$:0.01Fe in the vicinity of 242 K is not due to a ferroelectric phase transition, because: (i) the temperature dependence of the inverse value of the real part of the dielectric response does not follow the Curie–Weiss law in the vicinity of the anomaly and (ii) no dielectric hysteresis loops caused by spontaneous polarization were observed below 242 K. It is more likely that the anomaly existence and its form in the vicinity of 242 K speak in favor of an improper ferroelectric phase or antiferrodistortive transition. The next step in our studies was to see which structural changes occur in $CaTiO_3$:0.01Fe above and below the anomaly tempera-

ture. To this end, X-ray studies of $CaTiO_3$:0.01Fe were carried out at room temperature and at 200 K.

For the X-ray experiment, several small single crystals of perovskite were selected under an optical microscope. X-ray diffraction experiments were performed be means of a Bruker three-circle Smart APEX II X-ray diffractometer operated at 50 kV and 40 mA with MoKα radiation. The intensity dataset was collected during ~ 70 h in the regime of ω and φ scans, the frame width was 0.3° and counting time was 30 s per frame, $2\Theta_{max} = 112°$. The diffraction data obtained in the experiments were processed by the Bruker SAINT software. The data were integrated and corrected for absorption using an empirical ellipsoidal model by means of the Bruker programs APEX and XPREP. The structure of the compound was solved and refined with the program package Shelxl-97 [22]. Thermal displacement parameters of all atoms were refined in anisotropic approximation.

At room temperature $CaTiO_3$:0.01Fe is orthorhombic, space group $Pnma$ ($R_1 = 4.70\,\%$), with the unit-cell parameters $a = 5.4434(1)$, $b = 7.6437(2)$, $c = 5.3838(1)$ Å. The crystal structure of perovskite $CaTiO_3$:0.01Fe is rigid and consists of a framework of corner-sharing TiO_6 octahedra. The cuboctahedral cavities within the framework are occupied by Ca^{2+} cations. The structure of the mineral at 200 K does not change and can also be solved in the space group $Pnma$ ($R_1 = 4.72\,\%$) with the unit-cell parameters $a = 5.4416(2)$, $b = 7.6349(3)$, $c = 5.3772(2)$ Å. Since both diffraction datasets were collected from the same single crystal without changing its orientation, and the strategy of experiment was unvaried, we can speak about identical sets of diffraction data for the two temperatures studied. Because of the expected changes in symmetry in the vicinity of 240 K, basic sections of the reciprocal space for both temperatures were examined (Figs. 5 and 6) and it was clear that the diffraction patterns at 200 K contain very few additional reflections compared to the patterns measured at 293 K. For instance, such reflections as $(0\bar{6}9)$ and $(0\bar{6}\bar{9})$ are clearly visible in the diffraction patterns measured at 200 K. Nevertheless, the differences from the structural model of $CaTiO_3$:0.01Fe at 293 K were not large enough to state that the crystal structure of $CaTiO_3$:0.01Fe at 200 K could not be solved in the space group other than $Pnma$ (Table 1).

Analysis of atom coordinates, unit cell parameters, and anisotropic displacement parameters shows that the structure of $CaTiO_3$:0.01Fe does not experience significant changes with decreasing temperature. According to the single-crystal X-ray diffraction data, the crystal structure of perovskite at 200 K does not display any

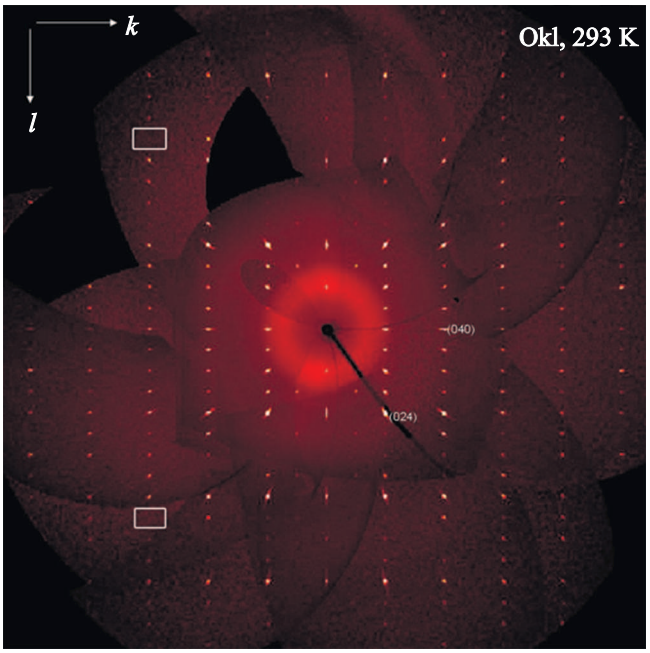

Fig. 5. (Color online) Reciprocal space reconstruction of the 0kl plane at 293 K in $CaTiO_3$:0.01Fe. Noted reflections are shown for the scale. The boxes mark areas in the reciprocal space where $(0\bar{6}9)$ and $(0\bar{6}\bar{9})$ reflections are located

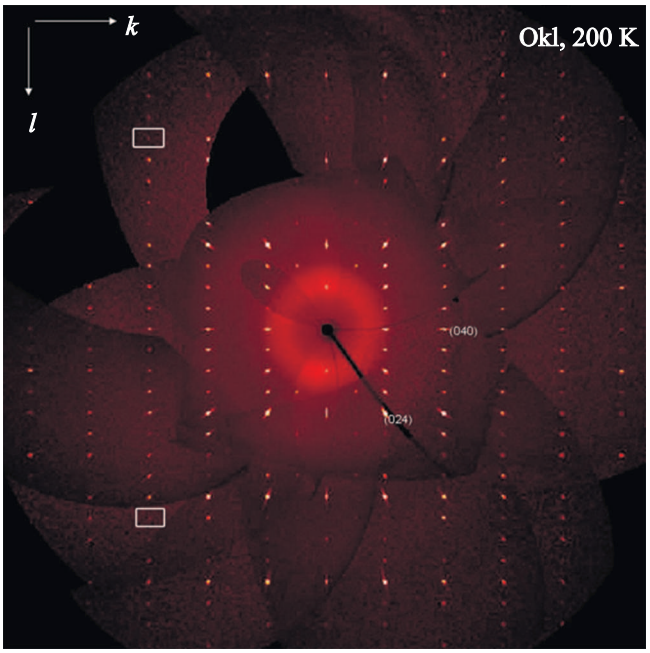

Fig. 6. (Color online) Reciprocal space reconstruction of the 0kl plane at 200 K in $CaTiO_3$:0.01Fe. Noted reflections are shown for the scale. The boxes mark areas in the reciprocal space where $(0\bar{6}9)$ and $(0\bar{6}\bar{9})$ reflections are located

Table 1. Crystallographic data and refinement parameters for the perovskite crystal at two temperatures*)

	200 K	293 K
Crystal data		
Ideal formula	$CaTiO_3$:0.01Fe	$CaTiO_3$:0.01Fe
Crystal system	Orthorhombic	Orthorhombic
Space group	*Pnma*	*Pnma*
Unit cell dimensions, a, b, c (Å)	5.4416(2), 7.6349(3), 5.3772(2)	5.4434(1), 7.6437(2), 5.3838(1)
Unit cell volume (Å^3)	223.402(15)	224.008(8)
Z	4	4
Calculated density (g/cm^3)	4.043	4.032
Absorption coefficient (mm^{-1})	5.815	5.799
Crystal size (mm^3)	$\sim 0.01 \times 0.002 \times 0.01$	$\sim 0.01 \times 0.002 \times 0.01$
Data collection		
Diffractometer	Bruker SMART APEXII	Bruker SMART APEXII
Temperature (K)	200	293
Radiation, wavelength (Å)	Mo-Kα, 0.71073	Mo-Kα, 0.71073
Θ range for data collection (deg)	4.64–56.00	4.63-55.74
h, k, l ranges	± 12, ± 17, ± 12	$-11 \to 12$, ± 17, $-11 \to 12$
Axis, frame width (deg), time per frame (s)	φ, ω, 0.3, 30	φ, ω, 0.3, 30
Reflections collected	17461	10189
Unique reflections (R_{int})	1528 (0.1201)	1518 (0.0442)
Unique reflections $F > 4\sigma(F)$	1271	1282
Data completeness to $\Theta_{\max}$ (%)	0.986	0.984
Structure refinement		
Refinement method	Full-matrix least-squares on F^2	Full-matrix least-squares on F^2
Weighting coefficients a, b**)	0.0580, 0.5769	0.0752, 0.4434
Extinction coefficient	0.010(4)	0.020(7)
Data/restraints/parameters	1528/0/29	1518/0/29
R_1 ($F > 4\sigma(F)$), wR_2 ($F > 4\sigma(F)$)	0.0472, 0.1253	0.0470, 0.1392
R_1 all, wR_2 all	0.0550, 0.1282	0.0547, 0.1443
Goodness-of-fit on F^2	1.098	1.145
Largest diff. peak and hole (e Å^{-3})	6.10, −4.77	6.682, −3.461

*) $R_{\text{int}} = (n/n-1)^{1/2}[F_0^2 - F_0(mean)^2]/\Sigma F_0^2$; $R_1 = \Sigma\|F_0| - |F_c\|/\Sigma|F_0|$; $wR_2 = \{\Sigma[w(F_0^2 - F_c^2)^2]/\Sigma[w(F_0^2)^2]\}^{1/2}$.
**) $w = 1/[\sigma^2(F_0^2) + (aP)^2 + bP]$, where $P = [\max(F_0^2, 0) + 2F_c^2]/3$; GooF $= \{\Sigma[w(F_0^2 - F_c^2)^2/(n-p)\}^{1/2}$, where n is the number of reflections and p is the number of refined parameters.

essential differences from that at room temperature and can be described by the same structural model. The picture derived from the measurements resembles the situation observed for the isotopic substitution of oxygen in $SrTiO_3$. The anomalies in physical properties attributed in [11] to a structural phase transition were not confirmed by the structural studies, which were explained by the fact that lattice distortions were so weak that they could not be distinguished by the available X-ray diffraction techniques. To clarify the nature of the observed anomaly in the dielectric response in the vicinity of 240 K, additional investigations are required by means of optical spectroscopic, synchrotron radiation techniques, etc.

To summarize, dielectric studies of $CaTiO_3$:0.01Fe have revealed an anomalous behavior of the dielectric response in the vicinity of 240 K (absent in chemically pure $CaTiO_3$) attributable, apparently, to the lattice instability. It has been shown that the dispersion in the dielectric response observed in the high-temperature region has a thermal-activation character and is likely to be induced by the existence of oxygen vacancies. The differences from the structural model of $CaTiO_3$:0.01Fe at 293 K observed in the X-ray studies were not large enough to detect deviations of the crystal structure of $CaTiO_3$:0.01Fe at 200 K from the *Pnma* model obtained for the room-temperature structure. The studies of magnetic properties of $CaTiO_3$:0.01Fe have shown that it is

a paramagnetic in the temperature interval from 4.3 to 300 K.

The authors wish to thank M.N. Murashko for the sample from collection and Yu.V. Pankova for the help during the experiments. The investigations were supported by Russian Science Foundation (# 14-12-00257).

1. *Light Scattering Near Phase Transitions*, ed. by H. Z. Cummins and A. P. Levanyuk, North-Holland, Amsterdam (1983), p. 414.
2. A. D. Bruce and R. A. Cowley, *Structural Phase Transition*, Taylor & Francis Ltd., London (1981), p. 410.
3. K. A. Müller and H. Burkard, Phys. Rev. B **19**, 3593 (1979).
4. W. Zhong and D. Vanderbilt, Phys. Rev. B **53**, 5047 (1996).
5. E. Cockayne and B. P. Barton, Phys. Rev. B **62**, 3735 (2000).
6. H. Moriwake, A. Kuwabara, C. A. J. Fisher, H. Toniguchi, M. Itoh, and I. Tanaka, Phys. Rev. B **84**, 104114 (2011).
7. V. V. Lemanov, A. V. Sotnikov, E. P. Smirnova, M. Weihnacht, and R. Kunze, Sol. State Comm. **110**, 611 (1999).
8. O. E. Kvyatkovskii, Phys. Sol. State **43**, 1401 (2001).
9. O. E. Kvyatkovskii, Sol. State Comm. **117**, 455 (2001).
10. A. Chandra, R. Ranjan, D. P. Singh, N. Khare, and D. Pandey, J. Phys.: Cond. Mat. **18**, 2977 (2006).
11. J. F. Scott, J. Bryson, M. A. Carpenter, J. Herrero-Albillos, and M. Itoh, Phys. Rev. Lett. **106**, 105502 (2011).
12. H. F. Kay and P. C. Bailey, Acta Cryst. **10**, 219 (1957).
13. T. Vogt and W. W. Schmahl, Europhys. Lett. **24**, 281 (1993).
14. T. Matsui, H. Shigematsu, Y. Arita, Y. Hanajiri, N. Nakamitsu, and T. Nagasaki, J. Nucl. Mater. **247**, 72 (1997).
15. B. J. Kennedy, C. J. Howard, and B. C. Chakoumakos, J. Phys.: Cond. Mat. **11**, 1479 (1999).
16. W. Cohran and A. Zia, Phys. Stat. Sol. **25**, 273 (1968).
17. V. Zelezny, E. Cockayne, J. Petzelt, M. F. Limonov, D. E. Usvyat, V. V. Lemanov, and A. A. Volkov, Phys. Rev. B **66**, 224303 (2002).
18. V. V. Lemanov, A. V. Sotnikov, E. P. Smirnova, and M. Weihnacht, Appl. Phys. Lett. **81**, 886 (2002).
19. H. Taniguchi, H. P. Soon, T. Shimizu, H. Moriwake, Y. J. Shan, and M. Itoh, Phys. Rev. B **84**, 174106 (2011).
20. D. O'Neill, R. M. Bowman, and J. M. Gregg, Appl. Phys. Lett. **77**, 1520 (2000).
21. D. Canil and A. J. Bellis, J. Petrology **48**, 231 (2007).
22. G. M. Sheldrick, *SHELXL-97*, University of Goettingen, Germany (1997), rel. 97–2.